A Superferric Quadrupole for use in an SRF Cryomodule

A. F. Zeller, J. C. DeKamp, A. Facco, T. L. Grimm, J. Kim, and R. Zink

[1]Abstract--A superferric quadrupole for use in a superconducting radio frequency (SRF) cryomodule has been designed and constructed. Even though the quad has a poor aspect ratio of length-to-aperture, the external fringe field is required to be small so that the SRF can operate at the high gradients required for the ISCL. Calculations of the external fringe fields required an iron flux clamp to obtain the necessary attenuation. Room temperature testing of the magnet confirmed the magnetic length.

Index Terms—Quadrupole, SRF, Superferric.

I. INTRODUCTION

The TRASCO project [1] of INFN (Istituto Nazionale di Fisica Nucleare, Italy) aims to study the physics and to develop the technologies needed to build an Accelerator Driven System (ADS) for nuclear waste transmutation. This project requires the development and prototyping of principal components of a 1 GeV, 30 mA proton accelerator. For the section from 5 to 100 MeV, an Independently phased Superconducting Cavity Linac (ISCL) is being considered [2], conceptually similar to those used for low energy heavy ions in many nuclear physics laboratories but dealing with a much higher beam intensity. One of the requirements of the TRASCO design was the linac capability of transporting the beam without losses even in case of one cavity failure. To ensure this a special lattice was studied, with a maximum energy gain per cavity limited to 0.5 MeV and with cylindrically symmetric (thus dipole free) reentrant cavities [3] as accelerating elements.

The linac lattice is based on a FODO structure with period $8\beta\lambda$. The focusing elements are short quadrupoles mounted inside cryostats; the number of cavities between quadrupoles increases with β. A schematic view of the building blocks is shown in Fig. 1. The required quadrupole gradient can be reached both by normal conducting and superconducting magnets. Superferric quadrupoles [4], combining a very compact size with a low power dissipation in the cryostat, have been found to be an excellent solution for this linac. A potential drawback is the residual magnetic field of the iron core, which must be shielded below 1 µT during cavity cool-down to prevent performance degradation of the nearby superconducting cavities. A superferric quadrupole prototype for the TRASCO ISCL has been designed and built at MSU-NSCL in the framework of a INFN-MSU collaboration on superconducting linac technologies.
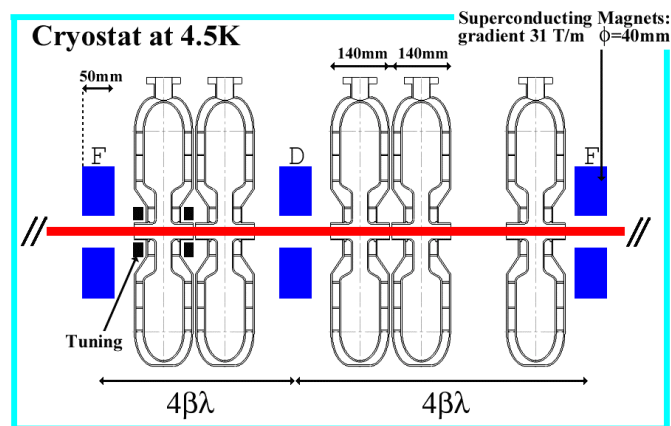

Fig. 1. ISCL layout: reentrant cavities and quadrupoles in the cryostat.

II. MAGNET DESIGN

Although the overall size of the magnet is small, the aspect ratio of length-to-diameter is relatively poor. The dimensions and gradient requirements are given in Table I. The ratio of the length-to-diameter is identical to that of the largest bore magnet used in the NSCL's recent A1900 upgrade [4]. The physical length of the quad was determined by scaling the A1900 quad to the required 50 mm effective length. The required current density was calculated in two dimensions. Because the fringe field has to be clamped, an iron flux clamp has been added to both sides of the magnet assembly. The flux shield was calculated in three dimensions with TOSCA [5]. The TOSCA results are shown in Fig. 2. The inset in Fig. 2 shows the tail of the fringe field in the region the cavity will occupy (100 mm from the effective edge of the magnet or 125 mm in the coordinates of Fig. 2). The calculated field at 125 mm is ~10 µT, which is satisfactory during operation because the Meissner Effect in the cavity provides sufficient shielding. A possible superconducting shield made of niobium can be placed at the end of the soft iron flux shield, or a Mu-metal shield can be placed entirely around the magnet, if necessary.

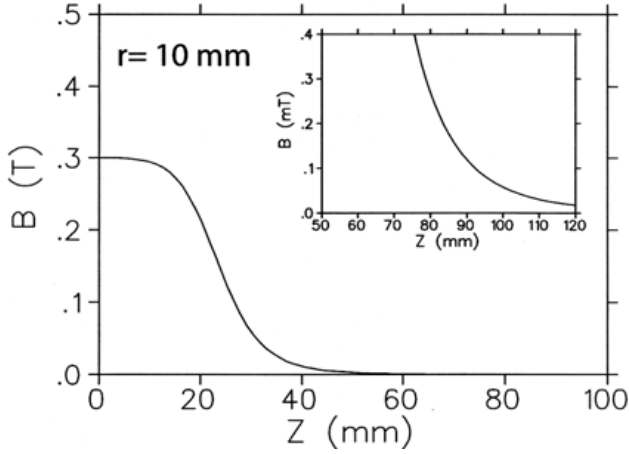| Property	Specification
Effective length	50 mm
Radius	20 mm
Gradient	31 T/m
Turns of 0.431 mm wire	78
Current (2-D calculation)	63 A

Fig. 2TOSCA calculations for the quadrupole with iron flux shield in place. Inset shows the region of the cavity. Calculations are for a radius of 10mm above the axis.

III. CRYOSTAT DESIGN

Since a major problem with SRF is contamination of the cavity and subsequent degradation, the intrinsically "dirty" potted coils and G10 insulation have to be in a separate insulation vacuum system. Fortunately, this doesn't represent too much of a problem because the flux shield can be easily enclosed in a helium-tight can. Since the magnet runs at less than 10% of short sample, the temperature margin for the conductor, $\Delta T_{critical}$, (4 K) is large. This means the cooling doesn't have to be complicated with cold helium gas being sufficient. Alternatively, cooling may be accomplished by conduction and the current leads brought into a reserve vessel to allow vapor cooling of the leads. Fig. 3 shows a schematic of the cryostat and flux shield.

IV. MAGNET CONSTRUCTION

The coils were wet-wound with Stycast® 2850 FT (Emerson and Cummings). The test coils were wound with 0.431 mm wire, surplus from the SSC. For production mode, it is likely that 0.3 mm, or smaller, will be used to reduce the current for lower helium consumption. Lowered helium consumption isn't particularly important, although, since the heat load is dominated by the cavity load. The yoke and pole tips were machined 1006 iron.

Coils are random-wound with a semi-automatic system that applies epoxy and positions the wire into the winding form. The operator only adjusts the height of the fixture to ensure complete filling of the form. After curing, the coils are removed from the form and shimmed into place around the pole tips with G10 shims. A bus ring provides solid support for the current leads. Fig. 4 shows the components of the magnet before assembly. The complete magnet is shown in Fig. 5.
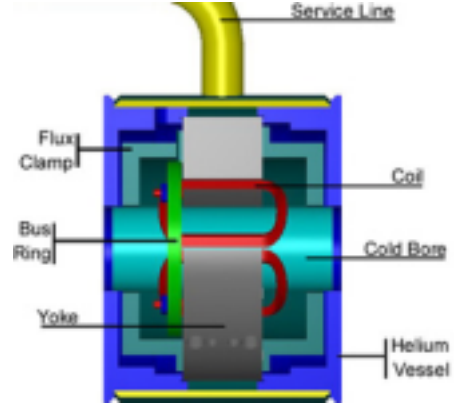

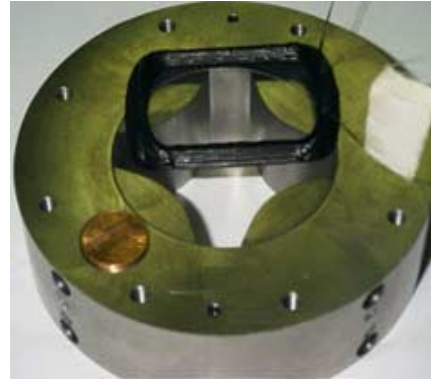Fig. 3. Cryostat with the quadrupole and flux shield in place.

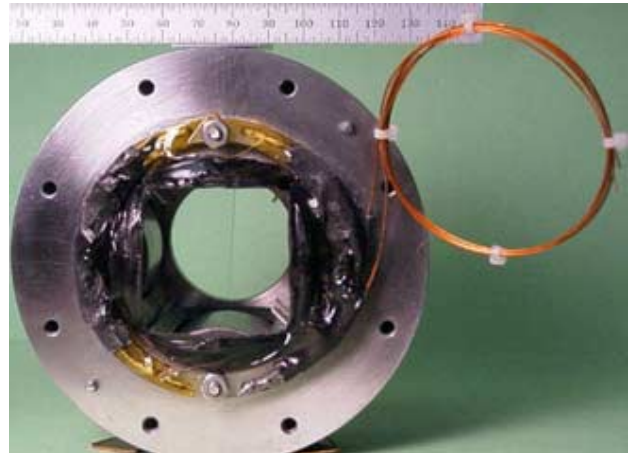Fig. 4. The yoke and coil with a penny shown for size.

Fig. 5. The complete magnet.

After assembly the flux clamp will be attached to the magnet, as shown in Fig. 6, although only one side is attached.
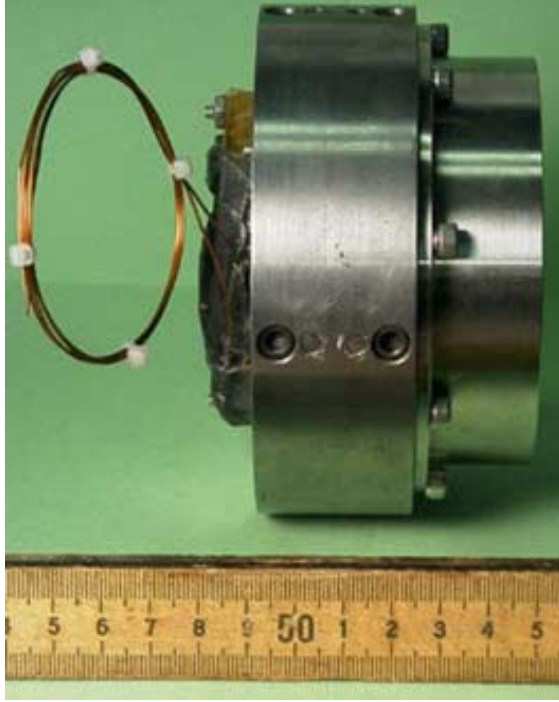

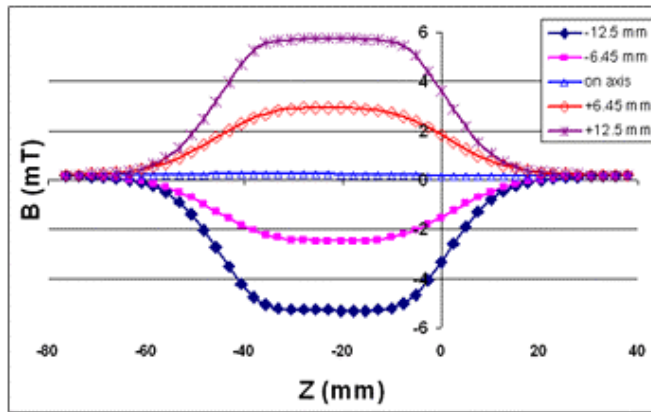Fig. 6. The complete magnet with one of the flux shields attached.

Fig. 7. Field maps at room temperature at a current of 1 A. The Z-axis has an arbitrary zero. Note the small positive field on axis due to probe alignment. This offset has been subtracted to obtain the transfer function.

V. Test Results

Because of laboratory reconstruction, a suitable test Dewar is presently not available at the NSCL. However, much can be determined from room temperature magnetic field mapping. The peak field at the pole tip is only about 0.6 T and, hence, unsaturated. Previous experience with these types of quadrupoles [4] indicates that the magnetic field properties do not change until the pole tips begin to saturate at about 1.5 T and thus room temperature results are a good prediction of cold testing. Therefore, a Hall probe mapping system was built to map the quad at room temperature. The probe was stepped through the magnetic field on axis, 6.45 mm and 12.5 mm above and below the central axis. A current of 1 Amp was used to limit heating of the coil and iron. The measured transfer function was 0.43 (T/m)/A. This results in a required current of 72 A for the full 31 T/m. A set of field maps is shown in Fig. 7.

The measured effective length is 50.8 mm, in good agreement with the scaled predictions. The estimated operating current of 63 A differs from the extrapolated 72 A by about 9%. This is a three dimensional effect; i.e., the result of the poor aspect ratio. An uncertainty of about 3 % in the measured length comes from the accuracy of positioning the probe at a known radius. The variance between the measurements at different radii yields an uncertainty of 2 %. Measured results for other quadrupoles in the lab typically have three-D effects on the order of 5 %, so the results are consistent with experience.

VI. Discussion

The quadrupole and flux clamp will be enclosed in the Dewar as shown in Fig. 3 and taken to INFN for cold testing. The first test will involve placing the assembly at the proper location next to the SRF cavity and attempting to operate the cavity at high gradient. If the cavity operates properly, then no further testing will be necessary. In the event of a decrease in performance, then an insert, which will allow field mapping, will be built to determine the field the cavity is experiencing. An appropriate modification of the iron shield or an additional shield will be added. Because of the expense of an additional niobium vessel and the associated complexity of the Dewar assembly, superconducting shielding will be used only if an appropriate Mu-metal and iron shield doesn't reduce the fringe field enough for high-electric field operation.

VII. References

[1] http://trasco.lnl.infn.it/
[2] A. Pisent, M. Comunian, A. Facco, M. Pasini, V. Zviagintsev, L. Celona, G. Ciavola, S. Gammino, G. Lamanna, "TRASCO 100 MeV high intensity proton linac", in *Proceedings of EPAC 2000*, Vienna, Austria, p. 857, 2000.
[3] A. Facco, V. Zviagintsev, B.M. Pasini, "A superconductive, low beta single gap cavity for a high intensity proton linac", in *Proceedings of the Linac 2000 Conference*, Monterey, USA, 2000.
[4] A. F. Zeller, et al, "Magnetic elements for the A1900 Fragment Separator", *Advances in Cryogenic Engineering*, vol. 43B, pp. 245-252, 1998.
[5] TOSCA, Vector Fields, Ltd.